Journal of Power Sources 195 (2010) 1971–1983

Contents lists available at ScienceDirect

Journal of Power Sources

journal homepage: www.elsevier.com/locate/jpowsour

High-efficiency power production from natural gas with carbon capture

Thomas A. Adams II, Paul I. Barton*

Process Systems Engineering Laboratory, Department of Chemical Engineering, Massachusetts Institute of Technology, Cambridge, MA, United States

ARTICLE INFO

Article history:
Received 28 August 2009
Received in revised form 15 October 2009
Accepted 15 October 2009
Available online 27 October 2009

Keywords:
Natural gas
Power
Solid oxide fuel cell
Carbon capture

ABSTRACT

A unique electricity generation process uses natural gas and solid oxide fuel cells at high electrical efficiency (74%HHV) and zero atmospheric emissions. The process contains a steam reformer heat-integrated with the fuel cells to provide the heat necessary for reforming. The fuel cells are powered with H_2 and avoid carbon deposition issues. 100% CO_2 capture is achieved downstream of the fuel cells with very little energy penalty using a multi-stage flash cascade process, where high-purity water is produced as a side product. Alternative reforming techniques such as CO_2 reforming, autothermal reforming, and partial oxidation are considered. The capital and energy costs of the proposed process are considered to determine the levelized cost of electricity, which is low when compared to other similar carbon capture-enabled processes.

1. Introduction

1.1. Natural gas combined-cycle plants

It is apparent that the introduction of aggressive controls on CO_2 emissions is imminent, whether through the proposed American Clean Energy and Security Act of 2009 [1] or some other means. To avoid the penalty for CO_2 emissions (carbon taxes, tariffs, etc.), industries that cannot avoid the use of fossil fuels may capture the CO_2 generated from their use and sequester it in subterraneous geological formations such as spent oil fields, saline aquifers, or other void spaces [2].

In the United States, natural gas accounts for approximately 30% of all electricity derived from fossil fuels (or about 22% from all sources) [3], but is only responsible for about 15% of all CO_2 emissions from that sector [4]. Because the gas-to-electricity process inherently generates less CO_2 per MW than from coal, policy makers anticipate that an increasing percentage of electricity will be derived from natural gas, relative to coal. For example, the current California Emission Performance Standard sets the limit for CO_2 emissions at 500 g kW^{-1} h^{-1} of electricity, equal to that of the average natural gas combined-cycle (NGCC) plant or about half of the amount produced by coal [5]. However, switching fuels to reduce emissions will only go so far, and carbon capture and sequestration (CCS) technology will still be needed in the face of anticipated regulations.

The NGCC process is rather simple. Natural gas is first desulfurized or otherwise cleaned (if not done prior to distribution) and then combusted in air at high temperature and pressure in a gas turbine, producing electricity. Waste heat from the exhaust is then recovered through the generation of high pressure steam, which then powers steam turbines for more electricity. The exhaust gases contain CO_2 and water diluted with a large amount of nitrogen originating from the air used for combustion. To recover the CO_2 from the nitrogen, CO_2 solvent-based absorption is usually preferred, which achieves approximately 90% recovery of the CO_2. The CO_2 is cooled and compressed to supercritical conditions, where it is distributed to an appropriate pipeline [6]. The de-carbonized exhaust gases are released to the atmosphere through the flue stack. Alternative strategies may involve reforming, shifting of the gas, and alternative means of CO_2 capture (as discussed in Section 3), but in general the combined cost and energy requirement of CO_2 capture is significant, causing as much as a 40% levelized cost of electricity increase [6].

1.2. Solid oxide fuel cells

The NGCC process can be modified by replacing the gas turbine with solid oxide fuel cells (SOFCs). SOFCs produce electricity by electrochemical means, rather than combustion. The SOFCs are constructed such that fuel provided to the anode can be kept separate from the oxygen source in the cathode, and only oxygen

Abbreviations: ACES, American Clean Energy and Security Act of 2009; ASU, air separation unit; ATR, autothermal reforming; CCS, carbon capture and sequestration; GT, gas turbine; HEN, heat exchanger network; HHV, higher heating value; HRSG, heat recovery and steam generation; IGCC, integrated gasification combined cycle; LCOE, levelized cost of electricity; NGCC, natural gas combined cycle; POX, partial oxidation; SOFC, solid oxide fuel cell; WGS, water–gas-shift.

* Corresponding author at: MIT 66-363, 77 Massachusetts Ave, Cambridge, MA 02139, United States. Tel.: +1 617 253 6526; fax: +1 617 258 5042.
E-mail address: pib@mit.edu (P.I. Barton).

0378-7753/$ – see front matter © 2009 Elsevier B.V. All rights reserved.
doi:10.1016/j.jpowsour.2009.10.046

ions transfer from the cathode to the anode side. This prevents the anode and cathode exhausts from mixing, and as a result, air can be used as the oxygen source without diluting the fuel exhaust with nitrogen. Thus, the fuel exhaust consists primarily of H_2O and CO_2 without N_2, allowing CO_2 recovery by condensation of the water, requiring little cost and power consumption. This avoids the energy-intensive CO_2 absorption step. Furthermore, the fuel cell itself is more efficient than combustion, since it is not subject to the thermodynamic limitations of a heat engine. Together, these drastically increase the electrical efficiency of the plant and avoid the large cost of electricity increase associated with CCS.

In this paper, we describe a novel process using natural gas and SOFCs which can generate electricity with 100% carbon capture at a very high electrical efficiency. Unless otherwise specified, we mean "electrical efficiency" to be the net electrical power output divided by the rate of thermal input of the fuel, using its higher heating value (HHV). We use the unit "%HHV" to denote this basis.

2. Process model

The proposed process to produce electricity and water from natural gas with zero atmospheric emissions is shown in Fig. 1, with example stream conditions in Table 1. The process can be broken into several sections: reforming, shifting, power generation, heat recovery, and CO_2 recovery.

2.1. Simulation basis

For the sample calculations presented herein, it is assumed that 4348 kmol h^{-1} of desulfurized natural gas is available at 30 bar and 38 °C, containing 93.9 mol% methane, 3.2% ethane, 0.7% propane, 0.4% *n*-butane, 1% CO_2, and the balance N_2. These are the same gas composition and inlet conditions used in the natural gas combined-cycle (NGCC) plant with CO_2 capture presented in the NETL's "Cost and Performance Base-line for Fossil Energy Plants. Volume 1: Bituminous Coal and Natural Gas to Electricity Final Report" [6]. Simulations were performed with Aspen Plus 2006.5, using the Peng–Robinson equation of state with the Boston–Mathias modification throughout the flowsheet, except: Redlich–Kwong–Soave EOS with predictive Holderbaum mixing rules for streams primarily containing CO_2 and H_2O well below the critical point of CO_2, and the electrolyte–NRTL model with Henry coefficients and electrolyte chemistry specifications obtained from the AP065 databank for CO_2/H_2O rich streams near the critical pressure of CO_2.

2.2. Steam reforming of natural gas

The reforming process involves reacting natural gas with steam at high temperatures (above 700 °C) to produce syngas (a gas rich in CO and H_2) through the following endothermic reactions:

$$C_nH_m + nH_2O \leftrightarrow nCO + (0.5m+n)H_2 \quad (1)$$

At atmospheric pressure, 99% conversion of methane can be achieved with H_2O:CH_4 molar ratios of 3:1 at about 750 °C. As the pressure increases, the temperature requirement for 99% conversion increases dramatically, approaching 1000 °C for 15 bar pressure [7]. In addition to the steam-reforming reaction, the water–gas-shift (WGS) reaction (2) and CO_2 reforming (3) reaction may take place [8]:

$$CO + H_2O \leftrightarrow CO_2 + H_2 \quad (2)$$

$$CH_4 + CO_2 \leftrightarrow 2CO + 2H_2 \quad (3)$$

It has commonly been assumed that power generation systems using SOFCs can be designed such that the steam-reforming process takes place inside the SOFC anodes simultaneously with the power generation reactions discussed in Section 2.4 [9–12]. Thermodynamically, this is advantageous since heat released by the electrochemical oxidation of CO and H_2 at high temperatures can be used to satisfy the high-temperature energy needs of the endothermic steam-reforming process directly. However, the deposition of carbon solids inside the anode is a major challenge to the feasible, long-term operation of an internal steam-reforming process [13–16]. Chemical equilibrium predictions show that for methane fuels above 400 °C, graphitic carbon exists as a stable, condensed phase [15]. As a result, the attainable fuel cell voltage decreases, causing a significant drop in the efficiency of the cell. Therefore, for natural gas fuels, steam reforming should occur upstream of the SOFC power generation section [16]. The use of pre-reformed methane has been experimentally demonstrated for a 5 kW scale SOFC power plant using pre-reformed LNG for 1000 h [17].

In the process of Fig. 1, natural gas is preheated to 615 °C and expanded to 12.5 bar through Turbine 1, producing power (see Section 2.8 for the methodology of selecting this pressure). The expanded natural gas (now at 550 °C) is fed to the pre-reformer with steam at a 2:1 C:H_2O ratio, which is sufficient for nearly complete conversion of ethane, propane, and butane while avoiding carbon deposition issues [8,18]. Because they have a relatively low concentration, the temperature drop of the bulk gas is relatively small. Therefore, the pre-reformer can operate adiabatically and still achieve high conversion. In the model for the pre-reformer, 99.9% conversion of C_nH_m for $n>1$ via Eq. (1) is specified. Methane steam reforming ($n=1$ in Eq. (1)) and Eqs. (2) and (3) are modeled as equilibrium reactions [8]. Note that the latter three only have a small impact on the reactor products, and that some methane is actually generated in this step [18].

The pre-reformer effluent is then heated to 950 °C and sent to the reformer. Because of a significant endotherm, heat is provided by integration with downstream sections of the plant, maintaining the reformer temperature at 950 °C. In the model for the reformer, methane steam reforming and Eqs. (2) and (3) are modeled as equilibrium reactions. It is assumed that the pre-reformer has a 0.4 bar pressure drop and the reformer has a 0.6 bar drop, which is consistent with existing industrial plants [8]. Lower pressures increase the methane conversion, but have a negative impact on the electrical efficiency of the downstream SOFCs, as described in Section 2.4.

Other types of reforming techniques, such as partial oxidation (POX) or autothermal reforming (ATR), may be used instead of steam reforming. These mature techniques are discussed in Section 2.9. This work considers the effect of their integration into the overall process, rather than the finer details of their implementation. For a closer look at these issues, we refer to Chapter 4 of Steynberg and Dry [8].

2.3. Syngas shifting

Though the use of natural gas-derived syngas as fuel for SOFCs has been previously proposed [13,19–22], recent studies have shown that syngas fuels have the same carbon deposition issues as methane fuel. Like methane, chemical equilibrium predictions show the formation of a stable, graphitic carbon phase when CO is present in the SOFC anode under normal operating conditions [15]. This is also true for a range of fossil fuel-derived syngas mixtures. Marquez et al. [23] confirmed experimentally that the presence of CO in the anode can cause both power loss and cell degradation, leading to a shorter lifetime and reduced efficiencies. Although Lim et al. [17] were able to run a SOFC for over a month on a syngas fuel, the effects of long-term exposure on the usable lifetime are still unclear. Furthermore, the authors showed that significantly more power was produced when running the fuel cell on H_2 rather than a mixture of H_2 and CO, highlighting the negative impact of

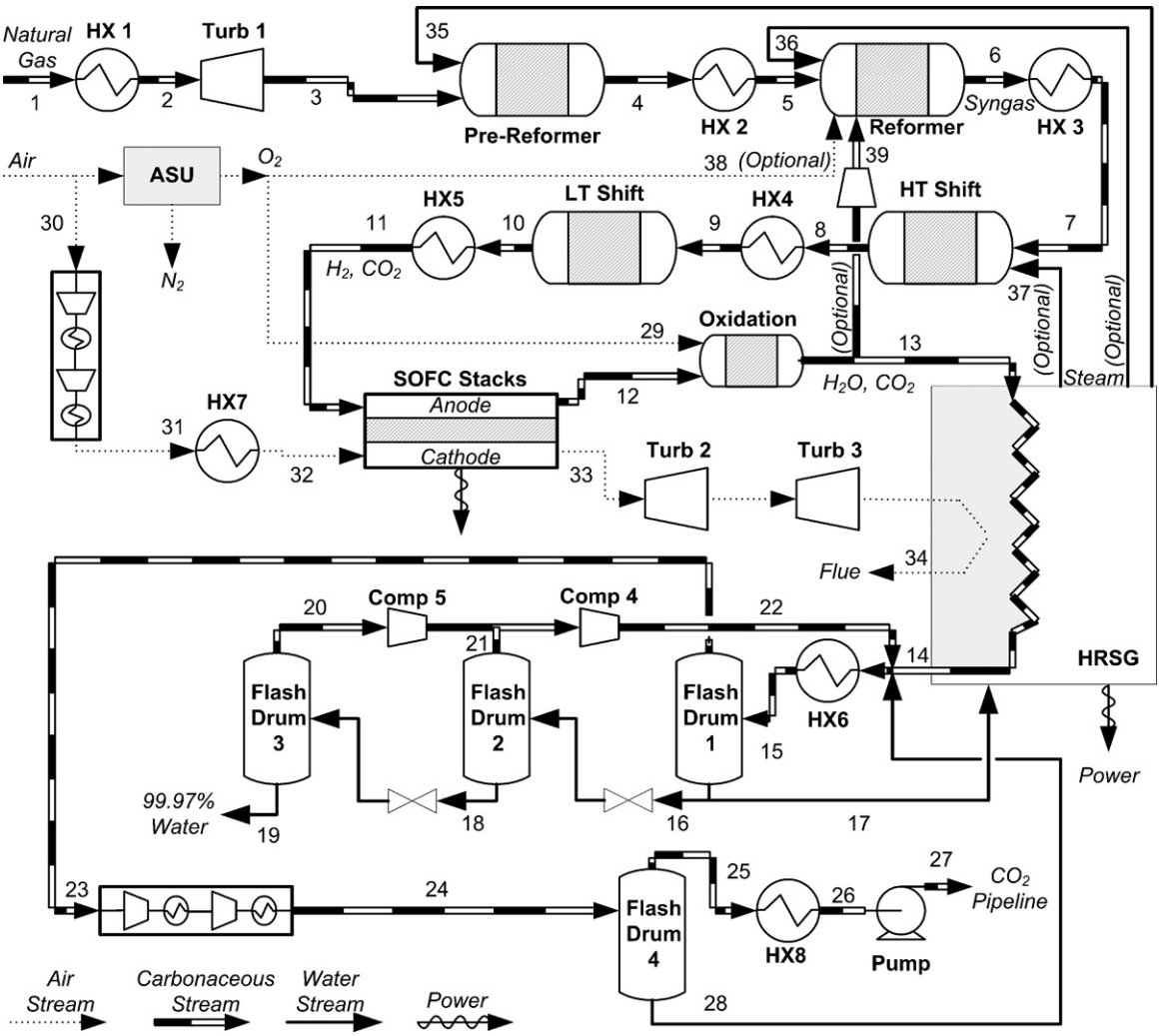

Fig. 1. The production of electricity and high-purity water from natural gas.

CO. However, it remains to be seen how this effect applies to other operating conditions.

In the water–gas-shift reaction (2), CO is converted to H_2 by reaction with steam. Although many variations are possible, the process of Fig. 1 utilizes two reactors in series: a high-temperature (300–350 °C) plug flow reactor and a low-temperature (200–250 °C) plug flow reactor, with an intermediate cooler. It is assumed that 80% conversion is achieved in the high-temperature reactor, and the low-temperature reaction approaches equilibrium, or about 96% conversion overall [6]. Though the actual conversion in the high-temperature reactor may vary with reactor dimensions, catalyst selection, and other factors [61], the impact on the plant electrical efficiency will be negligible if the second reactor approaches chemical equilibrium. Depending on the amount of steam used in the upstream reforming steps, additional steam is supplied to bring the H_2O:CO ratio up to 2:1 (via stream 37). The reactor effluent consists of >60 mol% H_2, with the balance mostly H_2O and CO_2 (the SOFC anode is tolerant of both). A pressure drop of 0.7 bar is assumed for each reactor.

2.4. Power generation

The SOFCs produce power through the following reactions:

$$H_2 + O^{2-} \rightarrow H_2O + 2e^- \quad \text{(anode)} \tag{4}$$

$$CO + O^{2-} \rightarrow CO_2 + 2e^- \quad \text{(anode)} \tag{5}$$

$$O_2 + 4e^- \rightarrow 2O^{2-} \quad \text{(cathode)} \tag{6}$$

Note that CO will be in very small quantities if the fuel is shifted syngas. The H_2 rich fuel is fed to the SOFC anode, while an oxygen source is provided in the cathode (usually air). Oxygen molecules encounter free electrons, producing ions (O^{2-}). The ions are conducted through the solid electrolyte and enter the anode, reacting with the fuel and releasing electrons. The electrons travel through the circuit, producing power, and return to the cathode. It is assumed that it is possible to consume up to 92% of the H_2 in the fuel cells [24].

In the example, the SOFCs operate at 10.1 bar and around 950 °C. Pressures up to 20 bar are technologically permissible, with higher pressures leading to somewhat higher efficiencies. However, efficiency losses become significant as the SOFC pressure decreases below 10 bar [24,25]. Ultimately, the design pressure should be chosen as part of a plant-wide optimization problem, where raising the system pressure increases the electrical efficiency of the SOFCs but decreases the conversion of methane in the reformers.

SOFCs typically operate at 800–1000 °C, with higher temperatures providing higher overall efficiency [24,25]. A portion of the heat of reaction is released as heat instead of electricity, and so inter-cooling stages are necessary to prevent temperatures from rising above 1000 °C. These inter-cooling stages can be heat-integrated with the steam reformer to provide a large portion of

Table 1
Example stream conditions for the process shown in Fig. 1 an assumed 86% fuel utilization of H_2 in the SOFCs.

	Stream												
	1	2	3	4	5	6	7	8	9	10	11	12	13
T (°C)	38	615	550	471	950	950	600	328	232	253	910	962	1413
P (bar)	30.0	30.0	12.5	12.1	12.1	11.5	11.5	10.8	10.8	10.1	10.1	8.7	8.7
F (kmol h^{-1})	4348	4348	4348	7127	7127	27,569	27,569	27,569	27,569	27,569	27,569	27,569	27,790
Vapor frac.	1	1	1	1	1	1	1	1	1	1	1	1	1
Mole fractions													
CH_4	93.9%	93.9%	93.9%	60%	60%	0.2%	0.2%	0.2%	0.2%	0.2%	0.2%	0.2%	19 ppm
C_2H_6	3.2%	3.2%	3.2%	19 ppm	19 ppm	5 ppm	5 ppm	5 ppm	5 ppm	5 ppm	5 ppm	5 ppm	49 ppb
C_3H_8	0.7%	0.7%	0.7%	4 ppm	4 ppm	943 ppb	943 ppb	943 ppb	943 ppb	943 ppb	943 ppb	943 ppb	9 ppb
C_4H_{10}	0.4%	0.4%	0.4%	3 ppm	3 ppm	798 ppb	798 ppb	798 ppb	798 ppb	798 ppb	798 ppb		
CO				0.3%	0.3%	11.8%	11.8%	2.4%	2.4%	0.6%	0.6%	848 ppm	8 ppm
CO_2	1%	1%	1%	4%	4%	4.8%	4.8%	14.3%	14.3%	16%	16%	16.5%	16.7%
H_2				10.1%	10.1%	52.1%	52.1%	61.6%	61.6%	63.3%	63.3%	8.9%	879 ppm
H_2O				25.2%	25.2%	30.9%	30.9%	21.5%	21.5%	19.7%	19.7%	74.2%	82.8%
N_2	0.8%	0.8%	0.8%	0.5%	0.5%	0.1%	0.1%	0.1%	0.1%	0.1%	0.1%	0.1%	0.2%
O_2				9 ppb	9 ppb	14 ppb	14 ppb	14 ppb	14 ppb	14 ppb	14 ppb		24 ppm
Ar				559 ppb	559 ppb	904 ppb	904 ppb	904 ppb	904 ppb	904 ppb	904 ppb	904 ppb	0.2%

	Stream												
	14	15	16	17	18	19	20	21	22	23	24	25	26
T (°C)	50	21	21	21	21	21	21	21	202	21	80	56	22
P (bar)	8.7	8.7	8.6	8.6	4.0	1.1	1.1	4.0	8.7	8.6	74.0	74.0	74.0
F (kmol h^{-1})	27,790	27,937	8850	14,283	8827	8812	16	22	38	4805	4805	4695	4696
Vapor frac.	0.17	0.17	0.00	0.00	0.00	0.00	1.00	1.00	1.00	1.00	1.00	1.00	0.00
Mole fractions													
CH_4	19 ppm	19 ppm	20 ppb	20 ppb			360 ppb	8 ppm	5 ppm	109 ppm	109 ppm	111 ppm	110 ppm
CO	8 ppm	8 ppm	7 ppb	7 ppb			100 ppb	3 ppm	2 ppm	49 ppm	49 ppm	50 ppm	50 ppm
CO_2	16.7%	17.1%	0.5%	0.5%	0.2%	650 ppm	97.8%	99.3%	98.6%	96.9%	96.9%	97.1%	97.1%
H_2	879 ppm	875 ppm	281 ppb	281 ppb	3 ppb		1 ppm	111 ppm	66 ppm	0.5%	0.5%	0.5%	0.5%
H_2O	82.8%	82.5%	99.5%	99.5%	99.8%	99.9%	2.2%	0.6%	1.3%	0.3%	0.3%	606 ppm	606 ppm
N_2	0.2%	0.2%	818 ppb	818 ppb	9 ppb		5 ppm	323 ppm	191 ppm	1.3%	1.3%	1.3%	1.3%
O_2	24 ppm	24 ppm	28 ppb	28 ppb			536 ppb	11 ppm	7 ppm	139 ppm	139 ppm	141 ppm	141 ppm
Ar	0.2%	0.2%	2 ppm	2 ppm	57 ppb		32 ppm	673 ppm	407 ppm	0.9%	0.9%	1%	1%

	Stream												
	27	28	29	30	31	32	33	34	35	36	37	38	39
T (°C)	39	56	80	15	398	910	962	50	550	950			
P (bar)	153.0	74.0	8.7	1.0	10.1	10.1	8.7	1.1	12.5	12.1			
F (kmol h^{-1})	4696	109	1442	43,390	43,390	43,390	35,812	35,812	2,283	12,000	0	0	0
Vapor frac.	Supercrit.	0	1	1	1	1	1	1	1	1			
Mole fractions													
CH_4	110 ppm	75 ppm							20 ppb	20 ppb			
CO	50 ppm	5 ppm							7 ppb	7 ppb			
CO_2	97.1%	88.2%	0.1%	300 ppm	300 ppm	300 ppm	363 ppm	363 ppm	0.5%	0.5%			
H_2	0.5%	4 ppb							282 ppb	282 ppb			
H_2O	606 ppm	11.5%	3%	1.1%	1.1%	1.1%	1.3%	1.3%	99.5%	99.5%			
N_2	1.3%	0.1%	1.8%	77.2%	77.2%	77.2%	93.5%	93.5%	818 ppb	818 ppb			
O_2	141 ppm	29 ppm	92%	20.8%	20.8%	20.8%	4%	4%	28 ppb	28 ppb			
Ar	1%	0.2%	3.1%	0.9%	0.9%	0.9%	1.1%	1.1%	2 ppm	2 ppm			

the high-temperature heat requirement. This is an advantage over other steam-reforming processes where a portion of the natural gas is combusted for the express purpose of providing high quality heat to the reformer, leading to an overall efficiency loss.

In the process of Fig. 1, shifted syngas is heated to 910 °C in HX5 and fed to the anode of the SOFC stack. Ambient air is compressed to 10.1 bar, preheated to 910 °C in HX7, and fed to the cathode. The fuel cells maintain separate anode and cathode exhaust streams, preventing the spent air from entering the fuel exhaust. Thus, the fuel exhaust essentially consists only of the waste gases (H_2O and CO_2) and some unreacted CH_4 and H_2.

The anode exhaust is fed to an oxidation reactor, where the unreacted H_2 (and any CO or CH_4 that may also remain) is reacted with a stoichiometric amount of O_2, creating heat, water and CO_2. In this example the oxygen source is provided at 92 mol% purity (the balance is N_2, Ar, and H_2O) by the cryogenic distillation of air in an air separation unit (ASU). The ASU model is described in detail in another work [26]. Because the amount of oxygen required is small, higher purity commercial sources may be more cost effective, particularly for smaller plants. The oxidation reactor exhaust is heat-integrated with the rest of the process.

The cathode exhaust is expanded to atmospheric pressure through a set of turbines, producing power. In this way, the air compressor, HX7, SOFCs and turbines form a Brayton cycle, improving the power output of the plant. The remaining heat in the expanded air stream is recovered in the HRSG.

The SOFC stacks were modeled as they were in previous works, assuming an ideal voltage of 0.96 V and an achieved voltage of 0.69 V applicable to pressures above 10 bar [26]. For pressures from 1 to 10 bar, a pressure-correction factor is applied [24], such that

Table 2
Summary of a heat exchanger network for the example conditions in Table 1.

		Duty (MW)	T in (°C)	T out (°C)	Cp,avail (MW °C^{-1})	Duty (MW)					
						I	II	III	IV	V	VI
Heat needs											
HX1	Natural gas preheat	38	38	615	0.07	3	1			27	7
HX2	Reformer preheat	56	470	950	0.12	16			16	22	2
	Reformer heating	257	950	950	0.00			209	47		
HX5	SOFC fuel preheat	178	253	910	0.27	39	5		29	89	16
HX7	SOFC air preheat	202	398	910	0.39	36			46	107	13
HRSG	Pre-reformer steam gen.	40	21	550	0.08	5	3			18	14
HRSG	Reformer steam gen.	266	21	950	0.29	42	1		32	151	40
HRSG	Bottoming steam gen.	290	43	550	0.57	52	15			154	70
Available sources											
HX3	WGS precooling	−193	950	216	0.26	193					
HX4	WGS interstage cool	−25	328	232	0.26		25				
SOFC	SOFC interstage cool	−209	950	950	0.00			209			
HRSG	Fuel exhaust cooling 1	−171	1413	958	0.38				171		
HRSG	Fuel exhaust cooling 2	−567	958	50	0.62					567	
HRSG	Air exhaust cooling	−162	588	50	0.30						162

The columns indicate the duty (in MW) of the heat exchanger connection between heat sinks and sources. For example, column I indicates that the WGS precooler provides 3 MW of heat to the natural gas preheater, 16 MW to the reformer preheater, 39 MW to the SOFC fuel preheater, etc., for a total of 193 MW of heat transfer through a total of seven connections. The "Cp,avail" column indicates the available heat capacity of each stream, given in terms of MW °C^{-1}. This analysis assumes a 0 °C ΔT_{min}.

the achieved voltage follows the following relationship:

$$V_{SOFC} = 2.62 \times 10^{-4} P^3 - 7.41 \times 10^{-3} P^2 + 7.49 \times 10^{-2} P + 0.421 \quad (7)$$

where V_{SOFC} is the voltage in V and P is the inlet pressure in bar.

2.5. Heat recovery and steam generation

The heat recovery and steam generation (HRSG) section of the plant integrates all of the heat sources and sinks throughout the plant. Some of this heat is used to produce the high temperature (950 °C), medium temperature (550 °C) and low-temperature (216 °C) steam required for the reforming, pre-reforming, and water–gas-shift units, respectively. The necessary water is provided by recycling a portion of the water recovered during CO_2 recovery (see Section 2.6), and contains a small amount of CO_2 (<1%). The remaining heat is used in a bottoming steam cycle to produce power. For this example, the steam cycle reaches 550 °C and 127 bar and uses a five-stage steam turbine with exit pressures of 28.2, 6.3, 1.4, 0.4, and 0.07 bar.

A heat exchanger network (HEN) for this example is described in Table 2. The HEN avoids temperature crossover, but assumes an idealized 0 °C ΔT_{min} for simplicity. This strategy provides an upper bound on heat integration capability and therefore helps to identify process configurations that are infeasible when heat integration is taken into account. More rigorous HEN synthesis methods are outside of the scope of this work.

It is assumed that all of the heat from the SOFC can be used toward high-temperature (950 °C) heat sinks. Since SOFC stacks are highly modular, this is technologically feasible by using a large number of inter-cooling stages. Alternatively, a tubular SOFC can be directly heat-integrated with a reformer by using a cluster of physically adjacent tubes, alternating between SOFC and reforming operations. Heat is then directly transferred from the SOFC tubes to the reformer tubes via radiation [20]. For the system shown in Table 2, this could provide up to 81% of the reformer heat load.

It is interesting to note how the fuel utilization of the SOFCs can affect the structure of the HEN. If the fuel utilization is raised, slightly more heat is produced in the SOFCs, but less recoverable heat is produced in the oxidizer, since less H_2 is available for oxidation. Overall, this reduces the amount of high quality heat for use in the reformer and reformer preheaters. For this process, no valid HENs were found for fuel utilizations above 86%, which was therefore chosen for the conditions shown in Table 1.

2.6. CO_2 recovery

The spent fuel gas, after heat recovery, consists primarily of CO_2 and H_2O at low temperature and about 8.6 bar. The CO_2 can be recovered through a three-stage flash cascade process described by Adams and Barton [27]. The gas stream is cooled to 21 °C and flashed in a drum at 8.6 bar. The liquid product contains water at about 99 mol% purity. A portion of this water is diverted to the HRSG for steam production for the pre-reforming, reforming and/or WGS operations as needed. The remaining water is flashed in two successive drums at 4 bar and 1 bar. Vapor products from these drums (rich in CO_2) are recompressed to 8.6 bar and recycled to the first drum. The liquid product from the last drum consists of >99.9 mol% purity water, which can be treated and used for other purposes.

The CO_2 rich vapor product from the first drum is compressed to 74 bar (near the critical point), cooled to 56 °C, and flashed in Drum 4. Most of the remaining water is recovered in the liquid phase and recycled to the HRSG for steam generation. The vapor product is condensed to a liquid and then pumped to supercritical pressures (153 bar) for transportation in a CO_2 pipeline.

2.7. Energy and environmental impact

For the conditions shown in Table 1, this process achieves 73.9%HHV electrical efficiency, producing a net 815 MW of electricity. As shown in Table 3, most of this is produced by the SOFC stacks, and only 96 MW are produced by the steam bottoming cycle. Although the power consumption of air compression for the SOFC cathode is large, it is mostly provided for by the recovery Turbines 2 and 3.

As a basis for comparison, consider Case 14 in Woods et al. [6]. This process represents a typical NGCC with CO_2 capture design, where natural gas is directly combusted with air in a gas turbine, and residual heat from the exhaust is captured in a bottoming steam cycle. This achieves 44%HHV efficiency and a net power output of 490 MW for the same input—significantly lower than the SOFC-based process. To capture the CO_2, an amine-based absorption process recovers CO_2 from the cooled flue gas, typically recovering about 90% of the CO_2. The unrecovered gases (including NO_X

Table 3
The power and environmental breakdown of the NG-SOFC processes presented in this work and the NGCC process with CO_2 capture presented in Case 14 of Woods et al. [6].

Methane reforming	This work	This work	This work	This work	NGCC [6]
Reformer type	Steam	CO_2 recycle	Partial oxid.	Autothermal	N/A
NG expander (Turb 1)	−5.4	−5.1	−5.4	−5.4	–
CO_2 recycle compressor	–	21.0	–	–	–
Power plant					
Air multi-stage compression	137.9	142.1	96.4	105.1	–
SOFC power produced	−751.7	−754.4	−562.6	−613.5	–
Gas turbine, including air compres.	–	–	–	–	−370.2
Air power recovery (Turb 2)	−57.0	−60.2	−39.4	−42.9	–
Air power recovery (Turb 3)	−65.8	−65.0	−45.4	−49.6	–
HRSG					
Total steam turbines	−97.8	−105.4	−167.3	−148.8	−149.9
Total pumps	1.5	1.5	2.4	2.1	5.0
CO_2 recovery					
CO_2/water separation (Comps 4 & 5)	0.1	0.1	0.1	0.1	–
Amine-based CO_2 recovery	–	–	–	–	9.6
CO_2 compression	9.4	9.1	9.5	9.4	15.0
Air separation					
Air separation power consumption	13.9	13.9	34.8	29.0	–
Net power output (MW)	815.0	802.4	676.8	714.4	490.5
HHV NG feed (MW)	1102	1102	1102	1102	1102
Plant electrical efficiency (%HHV)	73.9%	72.8%	61.4%	64.8%	44.5%
Emissions summary					
CO_2 in pipeline (kmol h^{-1})	4563	4564	4567	4563	4141
Carbon capture	100%	100%	100%	100%	91%
CO_2 emissions (tonne y^{-1})	0	0	0	0	151,000
NO_X emissions (tonne y^{-1})	0	0	0	0	115

For this work, cases using four different reforming techniques are presented. Some minor auxiliary loads of [6] were not included for this comparison. Negative values indicate power produced in MW, positive values indicate power consumed in MW.

and 10% of the CO_2) are emitted to the atmosphere through the flue.

The SOFC-based process has essentially zero atmospheric emissions. As shown in Table 3, nearly all of the carbon contained in the natural gas feed is captured, liquefied, and sent to the pipeline for sequestration. Only a slight amount of CO_2 escapes in the high-purity water product. It is permissible for some impurities to be present in the CO_2 sequestration stream, provided that the CO_2 purity is high enough. For this example, the water, N_2, and Ar concentrations are low enough for many pipelines in use in the industry [28]. Any NO_X gases that might be formed during this process (though neglected for this analysis) are also sequestered with the CO_2. Thus, no waste gases derived from the natural gas source are emitted to the environment.

Additionally, this process produces water, rather than consumes. Because all of the steam requirements are provided by recovery of water produced in the fuel cells, no freshwater needs to be added to the process. Rather, the recovered water is at very high purity, suitable for municipal wastewater treatment. For cooling requirements, cooling towers are typically preferred, which provide cooling by evaporating a supply of fresh water. The water produced in the power generation process can be recycled for this purpose, reducing the consumption of water drawn from the environment. Alternatively, if a waterless cooling system such as air-cooled exchangers is used (although at a larger energy penalty), no freshwater will be needed at all, and thus the plant will on the whole be water-positive. For this example, cooling towers were assumed for all cases. For the average gas-powered combined-cycle plant in the United States, cooling towers consume only about 0.4–0.5% of the total power output [57]. Therefore, the power consumption of the cooling towers was neglected for all cases in this analysis. The effect on the LCOE will not be significant.

The natural gas source in this example contained no other impurities, particularly sulfur. If other impurities were present, modifications will need to be made to the flowsheet, and is an area of future consideration.

2.8. Selection of steam-reforming conditions

The amount of methane conversion in the steam reformer has a significant effect on the efficiency of the plant as a whole. Insufficient conversion will result in both a reduced amount of hydrogen generation and a higher risk of carbon deposition, leading to lower SOFC power production and lower efficiencies. Conversion can be improved by reducing the reforming pressure and/or increasing the steam:methane ratio. However, low pressures in turn reduce the efficiency of the SOFC, and high steam ratios require a greater consumption of high-temperature heat and larger capital costs.

To determine the best operating conditions, the system of Fig. 1 was simulating using a range of pre-reformer pressures (the specified outlet pressure of Turb 1) from 8.5 to 15 bar, and reforming steam rates (the total flow of stream 36) ranging from 7000 to 13,000 kmol h^{-1} (resulting in steam:methane ratios of roughly 2:1–3.5:1). All downstream pressures and compressor specifications were adjusted accordingly. The resulting overall plant efficiencies are shown in Fig. 2. In general, increasing the reforming steam rate increased the electrical efficiency, but with diminishing returns. This increased efficiency is due to the increased conversion of methane in the reformer, producing more hydrogen, and thus a higher power output in the SOFC. For a given steam rate, however, an optimum pressure can be found, ranging from 11.5 to 12.5 bar in the range considered, quantifying the tradeoff between the pressure effects on the reformer conversion and the SOFC voltage. The chosen design spec for the case shown in Table 1 is 12.5 bar pressure and 12,000 kmol h^{-1} of reforming steam. This is the optimum operating condition, since higher steam flow rates demanded too much heat in the HRSG to produce and no suitable HEN could be found.

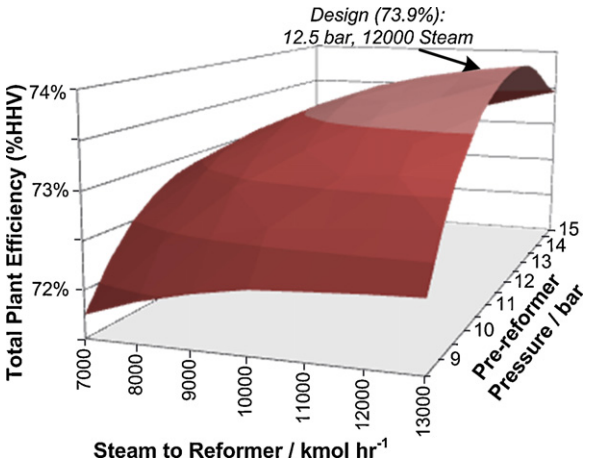

Fig. 2. Sensitivity of the efficiency of the SOFC-based process using steam reforming to the total flow rates of steam and the pressure of the pre-reformer. The reformer temperature is 950 °C. The optimal point and selected design points are annotated.

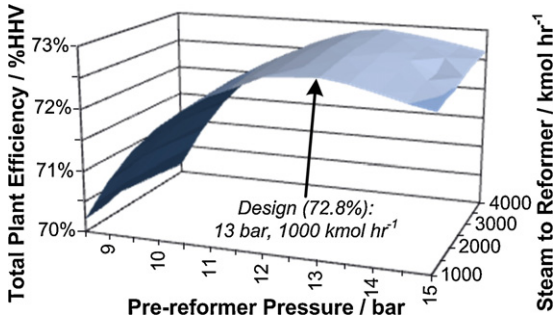

Fig. 3. Sensitivity of the total plant efficiency for the steam-reforming case with 40% recycle of the anode exhaust to the pressure of the pre-reformer and the flow rate of steam to the reformer.

2.9. Alternative reforming techniques

2.9.1. Anode exhaust recycling

The steam-reforming process, though thermally efficient, requires a significant amount of high-temperature heat transfer, both to the reformer itself and through the generation of steam at 950 °C. However, by recycling some of the high-temperature anode exhaust (optional stream 39 shown in Fig. 1), much of this burden can be alleviated. The exhaust is roughly 75% water and 25% CO_2, both of which can be used for methane reforming according to reactions (1) and (3).

As an example, 40% of the anode exhaust, after passing through the oxidation reactor and a recycle compressor, is recycled to the reformer. Potential operability problems associated with steam compression at high temperatures are ignored at present. Depending on the amount of reformer steam used, the generation of additional shifting steam (stream 37) may be avoided entirely. To find the optimal operating conditions, the pre-reformer pressure (the outlet pressure of Turb 1) and reforming steam rate (stream 36) are varied from 8.5 to 15 bar and 1000 to 4000 kmol h^{-1}, respectively, as shown in Fig. 3. Only pressure had a significant impact on the overall efficiency, with the most optimal pressure being 13 bar for nearly all steam rates in consideration. Thus, the final design condition was selected as 13 bar and 1000 kmol h^{-1} (a 92% reduction in high-temperature steam generation), which had an efficiency of 72.8%HHV. Higher steam rates had only a negligible impact on the efficiency. Selected stream conditions using this strategy are given in Table A of the supplementary material available on the journal website.

The resulting process was only slightly less efficient (~1 percentage point) than the steam-reforming case without recycle, as shown in Table 3, but required significantly less high-temperature steam generation, as shown in Table 4. Although the anode recycle case had generated about 8 MW more power from the SOFCs and the HRSG, this was insufficient to provide for the energy consumption of the anode exhaust recycle compressor, and thus is responsible for the small decrease in net power. Thus, the decision to recycle the anode exhaust must be determined by rigorous capital cost and operability considerations. For this case, it is unlikely that the capital cost savings from the smaller high-temperature heat exchanger will be large enough to justify the increased costs of the reformer, shift units, SOFCs, and oxidation reactor, which all must be enlarged to account for the increased volume due to recycle, as well as the cost of a new compressor capable of handling the high-temperature anode exhaust. It should also be noted that a valid HEN for this system could not be found, due to the significantly reduced availability of high-temperature heat from the anode exhaust which contributes to the bottoming cycle, SOFC preheating, and others. It may therefore be necessary to make other modifications, such as partial gas firing or oxidation to provide the necessary heat, generating less steam at the higher stages of the bottoming cycle, or introducing externally provided utilities. These techniques will reduce the electrical efficiency of the plant, and therefore will only be preferable to steam reforming when considerable capital cost benefits can be demonstrated. Such possibilities are outside the scope of this work.

2.9.2. Partial oxidation and autothermal reforming

To reduce the requirement of high-temperature reforming steam without recycling the anode exhaust, other reforming techniques can be considered. For example, partial oxidation (POX) can be employed to generate syngas from methane using oxygen over a suitable catalyst [29] according to:

$$CH_4 + 0.5\,O_2 \rightarrow CO + 2H_2 \qquad (\Delta H_{298\,K} = -36\,\text{kJ mol}^{-1}) \tag{8}$$

Because this reaction is exothermic, both methane preheating (with HX2) and external reformer heating become unnecessary. However, POX produces only two moles of hydrogen per mole of methane, compared to three moles for steam reforming, and thus less power is produced in the SOFCs downstream.

Without an external heating source, it is impractical to combine POX with steam reforming because the heat released by POX is too small to supply the heat needed for the steam-reforming reaction ($\Delta H_{298\,K}$ = 206 kJ mol^{-1}) and maintain a constant temperature [30]. For example, at standard conditions (ignoring the unfavorable equilibrium at low temperatures) 5.7 moles of CH_4 must be partially oxidized for each mole of CH_4 reformed. This ratio is even less favorable at high temperatures, rising to 22.9 at 950 °C as predicted thermodynamically using Aspen Plus. Instead, complete combustion of methane is needed to provide adequate heat, according to:

$$CH_4 + 2O_2 \rightarrow CO_2 + 2H_2O \qquad (\Delta H_{298\,K} = -890\,\text{kJ mol}^{-1}) \tag{9}$$

Using a restricted oxygen supply, a portion of the methane is fully oxidized, which provides ample heat to simultaneously reform the rest of the methane using steam. Overall, more methane is converted to H_2 than with POX, leading to higher power production in the SOFC. This is the principle of autothermal reforming (ATR). Compared to pure steam reforming, much less high-temperature steam is needed, and the temperature of that steam can be significantly lower, since the remaining high-temperature heat can be provided by combustion.

The process of Fig. 1 is modified slightly so that the steam reformer is replaced with either POX or ATR reactors (the pre-reformer remains the same). In either case, oxygen at 92% purity is provided from the air separation unit (stream 38), at the same

Table 4
Summary of water and oxygen use for various reforming techniques considered in this work.

Methane reforming Reformer type		This work Steam	This work Steam/CO_2	This work Partial oxid.	This work Autothermal	NGCC [6] None
Steam to pre-reformer (stream 35)	kmol h^{-1}	2272	2271	2272	2272	–
Pre-reformer steam temp.	°C	550	550	550	550	–
Steam to reformer (stream 36)	kmol h^{-1}	11,942	995	–	4230	–
Reformer steam temp.	°C	950	950	–	950	–
Oxygen to reformer (stream 38)	kmol h^{-1}	–	–	2778	2115	–
Anode exhaust to Ref. (stream 39)	kmol h^{-1}	–	12,304	–	–	–
Water–gas-shift						
Steam to WGS reactor (stream 37)	kmol h^{-1}	–	1657	5174	1554	–
Steam temperature	°C	–	216	216	216	–
Steam bottoming cycle						
Circulatory steam	kmol h^{-1}	17,623	19,067	30,254	26,912	49,827
Power generated	MW	−96	−104	−165	−147	−150
Amine CO_2 recovery						
Circulatory steam	kmol h^{-1}	–	–	–	–	15,510
Consumption and emissions						
Total steam in circulation	kmol h^{-1}	31,836	23,990	37,700	34,968	65,337
Net water loss to atmos.	kmol h^{-1}	–	–	–	–	2959
Recovered liquid water	kmol h^{-1}	8806	8816	8884	8865	–

The results are compared against the NGCC with 90% CO_2 capture process (Case 14 of Woods et al. [6]). Note that the NGCC process does not use reforming or shifting, and it uses a higher rate of circulatory steam used in the bottoming cycle due to different HRSG configurations and assumptions. Where applicable, stream numbers according to Fig. 1 are annotated in parentheses.

stream conditions as the oxygen fed to the oxidation reactor (stream 29). The steam fed to the reformer is reduced as needed, and the steam fed to the WGS reactors is adjusted accordingly to meet a 2:1 H_2O to CO ratio. A summary of the energetic and environmental breakdown for these two cases is shown in Table 3. Details on water circulation and emissions can be found in Table 4.

For the POX and ATR cases, the pre-reformer conditions remain the same as in the previous cases. However, the reformer itself operates adiabatically, and for the POX case, does not employ a preheater (HX2). For the ATR case, the reformer was modeled as an equilibrium reactor using reactions (1), (2), (3) and (9). For the POX case, it was assumed that 99% of the CH_4 is oxidized, and that the catalyst used for POX achieved 90% selectivity—that is, 90% of the oxidation occurs via (8), and the balance occurs via (9) [29]. Again, reactions (1), (2), (3) are assumed to be in equilibrium. HENs were found for both designs but are omitted for brevity. Oxygen for either POX and ATR (stream 38) is provided from the ASU.

Selected stream conditions for the POX design are given in Table B in the supplementary material. A stoichiometric amount of oxygen was fed to the reformer via stream 38 based on the methane in the feed. It is interesting to note that due to the small H_2O:C ratio, the steam-reforming and water–gas-shift reactions occur in reverse, but this is offset by the carbon dioxide reforming reaction. The net effect is that an additional 0.9% of the methane in the feed is converted to CO and water, resulting in 99.9% conversion. The pre-reformer pressure was subject to optimization in the 8.5–15 bar range, and it was found that 12.5 bar was optimal, as shown in Fig. 4. As the pressure decreases from 12.5 bar, the total plant power drops precipitously due mostly to the reduced performance of the SOFC unit. Above that, no further gains are seen in the SOFC output, due to the SOFC model assumption that negligible voltage improvements are seen above 10 bar.

Selected stream conditions for the ATR design are given in Table C in the supplementary material. Here, the flow rates of reforming steam (stream 36) and reforming oxygen (stream 38) are parameters, which affect the total plant efficiency as shown in Fig. 5. As was the case for pure steam reforming (see Section 2.8), increasing the steam flow rate generally increased the methane conversion and therefore the total plant efficiency, but with diminishing returns. For a given steam flow rate, however, an optimum oxygen flow rate can be found. Increasing the oxygen rate increases the amount of methane oxidized, which raises the temperature of

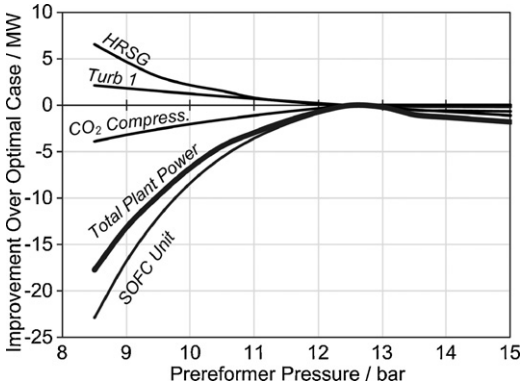

Fig. 4. The effect of the pre-reformer pressure on the power production or load on various sections of the plant for the case using partial oxidation, expressed as the amount of improvement over the optimal case (e.g., if the turbines produce more power than the optimal case, it is a positive number, and if a compressor uses more power, it is a negative number). The optimal case is 12.5 bar. The SOFC unit includes the air compressor, Turb 2 and Turb 3; the CO_2 compression line includes Turb 4, Turb 5, the CO_2 compressor and CO_2 pump.

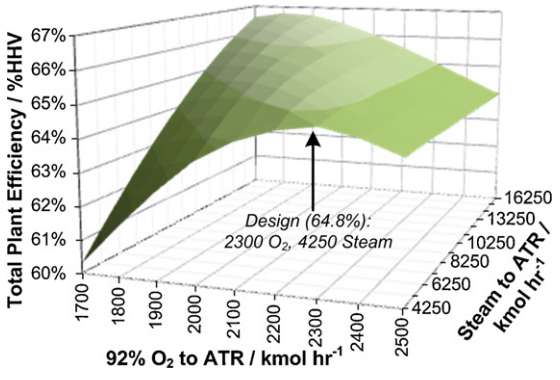

Fig. 5. The effect of reforming steam (stream 36) and oxygen (stream 38) total flow rates on the total plant efficiency for the ATR case.

Table 5
Summary of natural gas power plants using gas turbines (GT) or solid oxide fuel cells (SOFC).

External reforming?	Water–gas-shift?	CO_2 capture	Efficiency (%HHV)	References
Gas turbines only				
None	None	Single condenser after turbine	–	[37]
None	None	Absorption after turbine	40–45%	[6,31,32]
Steam	None	Single condenser after turbine	46%	[7]
ATR, steam	Before turbine	Absorption before turbine	40–41%	[7,35]
Combined gas turbine and SOFC				
None	None	None	56–72%	[12,36,38–43]
None	None	Absorption after GT/SOFC	54–59%	[34]
None	None	Single condenser after GT/SOFC	53%	[36]
Steam	None	None	41–42%	[17,44,45]
Steam	None	Absorption after GT/SOFC	–	[33]
ATR	Before turbine	Absorption before GT/SOFC	40%	[36]
SOFC only				
None	None	None	54–63%	[9,10][a]
None	After SOFC	Absorption after SOFC	63%	[11]
None	None	Single condenser after SOFC	61–62%	[11]
POX, ATR	None	None	–	[19,22]
Steam	None	None	54%	[13][a]
Steam	None	Single condenser after SOFC	44–58%	[20,21]
POX, ATR	Before SOFC	Multi-stage flash after SOFC	61–67%	This work
Steam	Before SOFC	Multi-stage flash after SOFC	73–74%	This work

[a] The referenced process did not consider a bottoming cycle to recover useful heat. For comparison purposes, it is assumed that the useful heat produced is recovered as electricity with 45% efficiency.

the reformer, and in turn promotes a more favorable equilibrium for the steam-reforming reaction. However, the counter-effect of increasing the amount of methane oxidized is that the amount of CH_4 used toward the electrochemical production of electricity in the fuel cell is reduced, being ultimately directed toward the less efficient bottoming cycle, resulting in a net reduction in total power.

The design selected for the ATR case uses an oxygen flow rate of 2300 kmol h^{-1} and a steam rate of 4250 kmol h^{-1}, reducing the reforming steam rate by about 65%. Although the efficiency of this point (64.8%HHV) is a bit lower than some points at higher steam rates (for example, 66.4%HHV at 1900 kmol h^{-1} O_2 and 14,250 kmol h^{-1} steam), the principle motive for using this ATR configuration is to reduce the amount of steam generation at 950 °C.

From these results, it is clear that the steam-reforming approach is significantly more energy efficient, having an electrical efficiency 9.1 percentage points higher than the ATR case and 12.5 points higher than the POX case. A small portion of this difference is due to the increased load on the air separation unit in the POX and ATR cases. However, it is mostly attributed to the greater amount of energy of the methane recovered (via H_2) using the more efficient SOFC rather than the bottoming cycle. Furthermore, this increased load on the bottoming cycle requires almost twice as much steam for that purpose in the POX and ATR cases. As a result, any benefit from the steam savings to the reformer by using POX or ATR techniques is counterbalanced by increased internal circulation in the bottoming cycle, resulting in about 25% more total steam circulation for the POX and ATR processes as a whole. Therefore, the POX or ATR designs should primarily only be considered when there is a significant capital or operability benefit from avoiding some or all of the high-temperature steam generation, or when heat integration of the reformer with the SOFCs or other sections of the plant is not practical.

3. Discussion

3.1. Comparison to other natural gas strategies

Many researchers and inventors have considered other variations using natural gas, as summarized in Table 5. Most use either a gas turbine (GT), SOFC, or a combination of the two. In general, combining a GT with an SOFC is a more thermodynamically efficient topping cycle strategy than a GT alone, and in turn, a SOFC-only system is the most efficient. CO_2 capture strategies can be broadly grouped into two categories: amine-based absorption and water condensing. Typically, amine-based absorption either takes place after the power generation step to recover CO_2 from N_2-rich exhaust gas [6,11,12,31–34], or, before the power generation step to recover CO_2 from syngas [7,35,36]. If the latter, a water–gas-shift step is necessary to generate the CO_2. These absorption processes usually require a significant amount of power, reducing the overall electrical efficiency of the plant by 7–17 percentage points [6,36].

The water condensing strategy is only applicable if the flue gas consists primarily of CO_2 and water. For combustion, this requires that the oxygen source is nearly pure so that N_2 does not dilute the waste stream. This can be provided by modifying the ASU to provide higher purity O_2 [7,58], or through future technologies such as ceramic autothermal recovery [59] or chemical looping combustion [60]. Although each strategy has tradeoffs between the CO_2 purity, recovery rate, cost, and efficiency, the overall penalties associated with generating the large amount of high-purity O_2 required for this approach are approximately the same as the penalties for amine-based CO_2 absorption methods. For SOFCs, as long as the anode and cathode exhaust gases are kept separate, air can be used as the oxygen source, avoiding these high costs. The water condensing step is usually specified as a single condenser [7,11,20,21,30,36,37,46], which requires significantly less power and capital than a typical multi-column absorption process with a specialized solvent.

The high efficiency of the proposed process is due mostly to the efficient use of SOFCs heat-integrated with steam reforming, and the use of a water condensing strategy for CO_2 recovery. The use of the water–gas-shift reactors also contributes to the efficiency of the plant, since SOFCs produce more power with H_2 fuel than with syngas [17]. As shown in Table 5, it achieves a higher efficiency than any CO_2 capture-enabled processes described in the literature, to the best of our knowledge. However, this comparison is only approximate, since differences in the inlet pressure, methane content, and impurities of the natural gas feedstock will affect the overall efficiency. Nevertheless, this process should remain competitive compared to currently known alternatives.

The process described in this paper is unique in several important ways. First, it is the only SOFC-based process (except for Franzoni et al. [36]) to use the reforming and water–gas-shift reactions upstream of the SOFC. If WGS is not used, the CO present in the fuel can cause carbon deposition and cell damage, as discussed in Sections 2.2 and 2.3. Thus, those processes are not practical for long-term industrial application.

The process of Franzoni et al. [36] does use both reforming and WGS reactions, but it uses an absorption process upstream of the power generation section. This contributes to a 17 percentage point drop in electrical efficiency (compared to an equivalent case without CO_2 capture). Furthermore, only about 90% capture is usually achievable through these methods. By comparison, the process of this paper reduces the energy penalty of capture to 1 percentage point, and achieves 100% CO_2 capture.

Third, the water condensing process to recover CO_2 used in this work utilizes a multi-stage flash cascade technique, which enables the recovery of high-purity water as well as CO_2. If a single-stage flash is used, particularly at higher pressures, the CO_2 content in the recovered water stream is high, giving lower CO_2 recoveries. Further details can be found in [27].

Other variations for natural gas plants involving SOFCs have been proposed. Geisbrecht and Williams [47] disclosed a process with SOFCs combined with polymer electrolyte fuel cells as a bottoming cycle, but this uses syngas for fuel and suffers from the same carbon deposition issues mentioned above. Micheli et al. [48] describe a comparable system combining SOFCs with molten carbonate fuel cells achieving about 64%HHV efficiency, but again this suffers from the same carbon issues and does not support CO_2 capture. Labinov et al. [49] propose separating syngas into CO and H_2 components by membranes and using separate SOFCs for each, but again, deposition issues remain.

3.2. Levelized cost of electricity

The levelized cost of electricity (LCOE) for the steam-reforming base case presented in this work (Table 1) is compared against the traditional NGCC case, both with and without carbon capture. These are derived from Cases 13 and 14 of Woods et al. [6] which use the same feed conditions as this work. Capital costs for the NGCC cases were taken from [6], which were derived from engineering estimates, quotes, and consultations.

Capital costs for the SOFC-based processes were scaled from appropriate estimates in [6] using the six-tenth's rule, where applicable. This applied to water handling systems, cooling towers, CO_2 compression, water–gas-shift units, air compressors, the HRSG (including steam turbines), the ASU, electrical transformers, catalysts, and other miscellaneous items. The remaining cost estimates were computed in-house using Aspen Icarus 2006.5 software. In cases where the size of the unit greatly exceeded the maximum size considered by the software, cost estimates from Seider et al. [50] are used to calculate the quoted purchase cost, which are then used by Icarus to compute the indirect and total costs of the unit. Small pumps, nozzles, and valves are ignored due to their negligible contribution to the capital cost of the plant, except where already included in [6] or in Icarus analyses by default.

The oxidation reactor is sized to achieve a superficial velocity of $1.0\,m\,s^{-1}$ with an aspect ratio of 1.79, which should be sufficient for nearly 100% oxidation of H_2 at high temperature in a catalytic bed [51]. The shell is constructed from Inconel to maintain stability at high temperature [52]. This yields cost estimates roughly 10 times that when using carbon steel, and so is a conservative estimate. Likewise, the reformer shell, natural gas preheater and reformer preheater are also constructed from Inconel.

The pre-reformer was modeled as an adiabatic packed-bed reactor. The size estimate was determined by integration of the PFR design equation using an appropriate rate law for ethane steam reforming and assuming 99.9% conversion of ethane [53]. The steam reformer is modeled as a large shell-and-tube heat exchanger, since heat must be continually provided by heat integration with downstream sources. In this case, heat sources pass through the shell side and reforming takes place in the catalyst-packed tubes [8]. In the absence of detailed design and cost information about how the SOFC and reformer might be heat-integrated, this approach is an acceptable estimate. The internal volume of the tubes is more than sufficient to meet the volume required for 99% conversion of methane, as estimated by the plug flow reactor design equation and an appropriate rate law [54], and is consistent with the size of industrial reformers [8]. Catalysts (and installation costs) for the pre-reformer and reformer are assumed to cost 10% of the total direct cost of the corresponding unit, and annual replacement costs are assumed to be the same as the quoted costs for the WGS catalyst (these are small contributions to the total).

The cost of the SOFCs is uncertain, and so $\$500\,kW^{-1}$ and $\$1000\,kW^{-1}$ cases are considered. These prices include the equipment, materials, installation, wiring, labor, and contingencies. The US DOE target price for 2010 is $\$400\,kW^{-1}$ [55], and so these correspond to reasonable and conservative estimates, respectively. Itemized summaries and other details about the cost analysis can be found in the supplementary material included in the online version of this journal.

The LCOEs are computed assuming: a grassroots/clear-field plant is constructed in 2012 (expressed in \$1Q2007); 20 year lifetime; 10% discount rate; 2.8% annual inflation rate; and 20% of the capital cost is paid in the first year, with a 20 year loan covering the balance, repaid in equal annual installments at 10% interest compounded annually. Assuming that carbon taxes are not taken into account, Table 6 shows a summary of the results. Cases 1–3 show results for the steam-reforming base case considering variations in SOFC price and whether or not CCS is employed. Cases 4 and 5 consider NGCC cases without and with carbon capture, respectively. Because of the uncertainty of constructing a plant around a new design, Case 1 (which is already conservatively estimated) is reconsidered assuming that all non-fuel operating costs are doubled (Case 6), or all capital costs are 25% or 50% greater (Cases 7 and 8, respectively). As a point of comparison, four cases using coal instead of natural gas are considered, each scaled to the same power output as Case 1. Cases 9 and 10 are subcritical pulverized coal plants without and with CCS, respectively, derived from Ref. [6]. Case 11 is a coal-based integrated gasification combined-cycle (IGCC) plant with CCS, also derived from Ref. [6]. Case 12 is a CCS-enabled, SOFC-based coal plant using similar concepts to this work [26].

One of the more interesting results of this analysis is that the conservative estimate for the CCS-enabled process of this work (Case 1) has a lower LCOE than even the NGCC case without CCS (Case 4), despite the fact that Case 1 has 4 times the capital cost of the NGCC case. This is attributed primarily to the large electrical efficiency of Case 1, brought about by the generation of H_2 and the use of SOFCs instead of a gas turbine. Thus, there is a significant financial incentive to construct this plant, even without carbon taxes. Also, it is interesting to note that constructing the SOFC-based without carbon capture (Case 3) only represents a LCOE savings of less than $0.2\,¢\,kW^{-1}\,h^{-1}$ (2%). Thus, the penalty for carbon capture in this case is reduced to a minimum. Furthermore, even assuming that the capital costs will be 50% more than anticipated (Case 8), the LCOE for this plant is still significantly lower than NGCC with CCS, even though the capital costs are roughly 3 times higher.

Putting aside various reasons for using one fuel type or another, traditional pulverized coal without CCS (Case 9) remains the cheapest option, as expected. However, once carbon taxes are imposed, this no longer is the case as will become apparent in the next sec-

Table 6
Cost summary for a variety of natural gas and coal plants, using various power supply methods, with or without carbon capture strategies.

	Case #					
	1	2	3	4	5	6
Fuel type	NG	NG	NG	NG	NG	NG
Power supply	SOFC	SOFC	SOFC	Gas turb.	Gas turb.	SOFC
SOFC cost ($\$\,kW^{-1}$)	\$1,000	\$500	\$1,000			\$1,000
Carbon capture	100%	100%	0%	0%	90%	100%
Sensitivity case						2 × operating
Electrical efficiency (%HHV)	74%	74%	75%	51%	44%	74%
Thermal input (MW)	937	937	937	937	937	937
Power output (MW)	693	693	701	476	410	693
CO_2 emitted ($kg\,MWh^{-1}$)	0	0	244	361	42	0
CO_2 sequestered ($tonne\,y^{-1}$)	1,495,325	1,495,325	–	–	1,356,746	1,495,325
Total capital cost (\$1000s)	\$1,239,482	\$863,638	\$1,212,547	\$313,940	\$567,859	\$1,239,482
Total oper. cost ($\$1000s\,y^{-1}$)	\$205,647	\$205,647	\$205,384	\$200,245	\$206,658	\$219,716
LCOE ($¢\,kWh^{-1}$)	6.45	5.74	6.32	6.67	8.79	6.73

	Case #					
	7	8	9	10	11	12
Fuel type	NG	NG	Coal	Coal	Coal	Coal
Power supply	SOFC	SOFC	Boiler	Boiler	IGCC	SOFC
SOFC cost ($\$\,kW^{-1}$)	\$1,000	\$1,000				\$1,000
Carbon capture	100%	100%	0%	90%	94%	100%
Sensitivity case	1.25 × capital	1.5 × capital				
Electrical efficiency (%HHV)	74%	74%	37%	25%	38%	45%
Thermal input (MW)	937	937	1,883	2,782	1,814	1,546
Power output (MW)	693	693	693	693	693	693
CO_2 emitted ($kg\,MWh^{-1}$)	0	0	855	126	53	0
CO_2 sequestered ($tonne\,y^{-1}$)	1,495,325	1,495,325	–	6,914,571	5,010,571	4,113,998
Total capital cost (\$1000s)	\$1,549,352	\$1,859,223	\$1,118,972	\$2,090,319	\$1,633,550	\$1,877,103
Total oper. cost ($\$1000s\,y^{-1}$)	\$205,647	\$205,647	\$152,105	\$238,768	\$167,227	\$144,769
LCOE ($¢\,kWh^{-1}$)	7.04	7.63	5.16	8.73	6.44	6.45

Fuel prices are the same as those in Ref. [6], that is, \$6.75/MMBtu for natural gas and \$1.80/MMBtu for coal.

tion. For the CCS-enabled processes, the IGCC with CCS case (Case 11) and the SOFC-based coal process with CCS (Case 12) have essentially the same LCOE as Case 1. This interesting result shows that at this particular scale (~700 MW), the choice of fuel is not immediately clear and will depend highly on other factors such as carbon tax policy, fuel price stability, reliability, and confidence in the assumptions used to generate these estimates. A rigorous analysis of these factors is left to future work.

3.3. Introduction of carbon taxes

The American Clean Energy and Security Act of 2009 (ACES) has been introduced to the US Congress, which describes, in part, a regulatory system for the gradual reduction of CO_2 emissions using a "cap-and-trade" methodology [1]. The bill is complex, and since it is still under debate it is likely to see substantial revisions if it becomes law. Therefore, the effects on the LCOE for Cases 1–12 are considered according to the following sets of rules and assumptions which approximate the relevant provisions in the bill: (1) all plants begin operation in January 1, 2012 and are permitted sometime between 2010 and 2011, meaning that no emissions credits for existing coal plants will be given under §783. (2) Since the supply of carbon credits available on the open market will be limited and decreasing, it is assumed that each plant will only be able to obtain credits in proportion to its average CO_2 emissions for the fuel type and the total allocations that will be distributed in each year according to §721. Assuming a 0.7% annual growth rate of electricity production [56] and other assumptions, the maximum amounts of credits obtainable for a gas or coal plant are shown in the supplementary material. (3) If more credits are needed than are available, carbon offsets are purchased at a rate of 1.5 times the market price of a carbon credit allowance (note that otherwise, the bill states that fines would be paid to the government at twice the price of a carbon credit). Banking and borrowing is ignored. (4) Since §782 calls for a certain percentage of carbon credits to be distributed freely to plants with at least 50% carbon capture constructed before 2020, it is assumed that 1000 MW of power are produced in the U.S. from plants with 50% capture in 2012, increasing at a rate of 10% per year. This results in the schedule of carbon credits given freely to CCS-enabled plants shown in the supplementary material. These credits are sold at the market rate if they are in excess. The derivation for these numbers and more details about this model are included in the online supplementary material.

Using this model, the LCOEs for Cases 1–12 are computed as a function of the average lifetime cost of a carbon credit, as shown in Fig. 6. In general, it becomes obvious that the costs of plants without CCS capability increase very quickly with the cost of a carbon credit, while the cost for the NGCC and IGCC cases increase slowly (due to incomplete capture of CO_2). The SOFC-based cases do not increase, but rather decrease slightly since free credits given under §782 are sold for additional revenue. Looking for a moment only at natural gas cases, and ignoring the $\$500\,kW^{-1}$ Case 2, the conservative Case 1 remains the cheapest option for all carbon prices above $\$5\,tonne^{-1}$, thus creating a basic minimum incentivisation price necessary to encourage CCS under the context of the new process presented in this work. Even taking the very-conservative-case scenario where capital costs are 1.5 times higher (Case 8), the incentivisation price only needs to be about $\$17\,tonne^{-1}$ for plants of the same scale (693 MW). Below $\$17\,tonne^{-1}$, one would choose to construct an NGCC plant with-

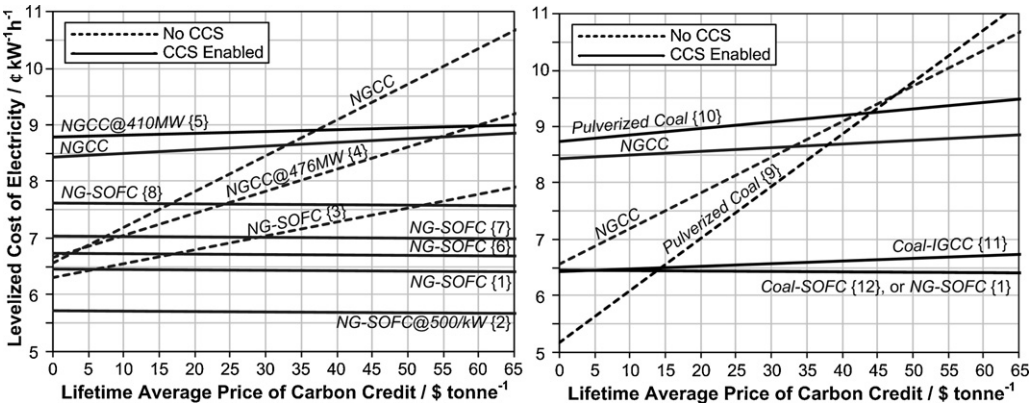

Fig. 6. LCOE predictions for various power plants under the ACES cap-and-trade scenario. Numbers in braces correspond to the case number in Table 6 where applicable. All plants are scaled for 693 MW power output unless otherwise specified. All SOFC costs are \$1000 kW^{-1} unless otherwise specified. The lines for Cases 1 and 12 are indistinguishable at this scale.

out CCS. Without SOFC technology, the incentivisation price climbs to \$33 $tonne^{-1}$.

Comparing the natural gas plants to coal plants of the same scale (693 MW), pulverized coal without CCS remains the cheapest option up to about \$15 $tonne^{-1}$. Above this price, one would choose either fuel (coal or natural gas) with the SOFC power strategy discussed in this paper. The coal-based IGCC process is another option, but it diverges from the fuel cell processes at higher carbon prices because it achieves only about 94% carbon capture, so credits must still be purchased for the remaining 6%. However, the difference between the IGCC and SOFC process may become lesser or greater depending on the scale, fuel composition, fuel price, and a wide range of factors. Without gasification or SOFC technology, the incentivisation price to build a CCS-enabled pulverized coal plant must be about \$45 $tonne^{-1}$, and that is only if switching to natural gas is not an option. Otherwise, one would construct a NGCC plant with CCS if the price were above \$37 $tonne^{-1}$.

4. Conclusions

A process to produce electricity and high-purity water with high efficiency (74%HHV) and zero atmospheric emissions (100% carbon capture) has been described. This is achieved using solid oxide fuel cells fueled by hydrogen derived from reformed, shifted natural gas, and a multi-stage flash cascade process to recover CO_2 and H_2O from the exhaust gases. The dual-effect of high efficiency and 100% carbon capture makes it the most cost-effective means of green power generation out of any of the natural gas processes considered in this study. With this new technology, the carbon price needed to incentivise carbon capture can be reduced by roughly 45–80%, even when considering options such as pulverized coal power generation without CCS. This will greatly encourage the use of carbon-capture technology while significantly reducing the cost impact to the consumer.

Acknowledgements

We thank Randall Field (MIT), Valerie Karplus (MIT), and the engineers at BP for their helpful insights. This project was conducted as a part of the BP-MIT Conversion research program.

Appendix A. Supplementary data

Supplementary data associated with this article can be found, in the online version, at doi:10.1016/j.jpowsour.2009.10.046.

References

[1] H.A. Waxman, E.J. Markey, The American Clean Energy and Security Act of 2009, Proposal to US House of Representatives, H.R. 2454 (July 6, 2009).
[2] H.J. Herzog, D. Golomb, Carbon capture and storage from fossil fuel use, in: C.J. Cleveland (Ed.), Encyclopedia of Energy, Elsevier Science, New York, 2004, pp. 277–287.
[3] Energy Information Administration, Electric Power Annual 2007, US DOE/EIA-0348 (2007), January 2009.
[4] J. Conti, G.E. Sweetnam, et al., Emissions of Greenhouse Gases in the United States 2007, US DOE/EIA-0573(2007), December 2008.
[5] S. Wartmann, P. Jaworski, S. Klaus, C. Beyer, Scenarios on the Introduction of CO_2 Emission Performance Standards for the EU Power Sector, Ecofys Germany GmbH, January 2009.
[6] M.C. Woods, P.J. Capicotto, J.L. Haslbeck, N.J. Kuehn, M. Matuszewski, L.L. Pinkerton, M.D. Rutkowski, R.L. Schoff, V. Vaysman, Cost and Performance Baseline for Fossil Energy Plants. Volume 1: Bituminous Coal and Natural Gas to Electricity Final Report, DOE/NETL-2007/1281, Revision 1, August 2007.
[7] N. Zhang, N. Lior, J. Eng. Gas Turbines Power 130 (2008) 051701-1–151701-11.
[8] K. Aasberg-Petersen, T.S. Christensen, I. Dybkjær, J. Sehested, M. Østberg, R.M. Coertzen, M.J. Keyser, A.P. Steynberg, Synthesis gas production for FT synthesis, in: A. Steynberg, M. Dry (Eds.), Fischer–Tropsch Technology, Elsevier, Amsterdam, 2004.
[9] Y. Lu, L. Schaefer, J. Power Sources 135 (2004) 184–191.
[10] J.A. Matelli, E. Bazzo, J. Power Sources 142 (2005) 160–168.
[11] S. Campanari, J. Power Sources 112 (2002) 273–289.
[12] W.F. Domeracki, W.L. Lundberg, T.E. Dowdy, J.M. Linder, Integrated gas turbine solid oxide fuel cell system, US Patent 5,413,879 (1995).
[13] R. Peters, E. Riensche, P. Cremer, J. Power Sources 86 (2000) 432–441.
[14] K.M. Walters, A.M. Dean, H. Zhu, R.J. Kee, J. Power Sources 123 (2003) 182–189.
[15] R.J. Kee, H. Zhu, A.M. Sukeshini, G.S. Jackson, Combust. Sci. Technol. 180 (2008) 1207–1244.
[16] M. Naponen, M. Halinen, J. Kiviaho, J. Saarien, J. Fuel Cell Sci. Technol. 3 (2006) 438–444.
[17] T.-H. Lim, R.-H. Song, D.-R. Shin, J.-I. Yang, H. Jung, I.C. Vinke, S.-S. Yang, Int. J. Hydrogen Energy 33 (2008) 1076–1083.
[18] T.S. Christensen, Appl. Catal. A: Gen. 138 (1996) 285–309.
[19] J. Kiviaho, M. Halinen, M. Noponen, J. Saarinen, P. Simell, R. Rosenberg, Trans. ASME 4 (2007) 392–396.
[20] E. Riensche, E. Achenbach, D. Froning, M.R. Haines, W.K. Heidug, A. Lokurlu, S. von Andrian, J. Power Sources 86 (2000) 404–410.
[21] T.R. Galloway, Process and system for converting carbonaceous feedstocks into energy without greenhouse gas emissions, US Patent App. 2007/0099038 A1 (2007).
[22] K. Ohsaki, M. Okada, S. Kazumi, Fuel cell power generating system, US Patent 4,988,580 (1991).
[23] A.I. Marquez, T.R. Ohrn, J.P. Trembly, D.C. Ingram, D.J. Bayless, J. Power Sources 164 (2007) 659–667.
[24] EG&G Technical Services, DOE/NETL Fuel Cell Handbook, seventh ed., November 2004.
[25] L. Duan, Y. Yang, R. Lin, Int. J. Thermodyn. 10 (2007) 61–69.
[26] T.A. Adams, P.I. Barton, Clean coal: high efficiency power plant with carbon capture, submitted for publication.
[27] T.A. Adams, P.I. Barton, Systems and methods for the separation of carbon dioxide from water, US Patent App. 12/434486 (2009).
[28] E. deVisser, C. Hendriks, M. Barrio, M.J. Mølnvik, G. deKoeijer, S. Liljemark, Y.L. Gallo, Int. J. Greenhouse Gas Control 2 (2008) 478–484.
[29] O. Deutschmann, L.D. Schmidt, Two-dimensional modeling of partial oxidation of methane on rhodium in a short contact time reactor, in: Proceedings of the 27th Symp. (Int.) Combust., 1998, pp. 2283–2291.
[30] W. Han, H. Jin, W. Xu, Energy 32 (2007) 1334–1342.

[31] G.P. Hammond, O. Akwe, S. Serge, Int. J. Energy Res. 31 (2007) 1180–1201.
[32] B.F. Möller, M. Genrup, M. Assadi, Energy 32 (2007) 353–359.
[33] B. Varatharajan, C. Balan, D. Dey, Integrated fuel cell hybrid power plant with controlled oxidant flow for combustion of spent fuel, US Patent App. 2005/0079395 A1 (2003).
[34] P.L. Micheli, M.C. Williams, E.L. Parsons, Indirect-fired gas turbine bottomed with fuel cell, US Patent 5,449,568 (1995).
[35] J.-M. Amman, M. Kanniche, C. Bouallou, Clean Technol. Environ. Policy 11 (2009) 67–76.
[36] A. Franzoni, L. Magistri, A. Traverso, A.F. Massardo, Energy 33 (2008) 311–320.
[37] T. Griffin, S.G. Sundkvist, K. Asen, T. Bruun, J. Eng. Gas Turb. Power 127 (2005) 81–85.
[38] M. Granovskii, I. Dincer, M.A. Rosen, J. Fuel Cell Sci. Technol. 5 (2008) 031005-1–131005-9.
[39] S.H. Chan, H.K. Ho, Y. Tian, J. Power Sources 109 (2002) 111–120.
[40] A.D. Rao, G.S. Samuelsen, J. Eng. Gas Turb. Power 125 (2003) 59–66.
[41] M.J. Skowronski, Power generation system utilizing turbine and fuel cell, US Patent 5,811,201 (1998).
[42] T. Tsuji, Fuel cell device and power generating facility, US Patent App. 2004/0241514 A1 (2004).
[43] G. Angelino, C. Invernizzi, P. Iora, J. Power Energy 222 (2008) 371–379.
[44] R.S. Bunker, C. Balan, Cooled turbine integrated fuel cell hybrid power, US Patent 7,153,599 (2006).
[45] H. Shingai, H. Nishigaki, Fuel cell/gas turbine combined power generation system and method for operating the same, US Patent 5,482,791 (1996).
[46] R.E. Anderson, H. Brandt, F. Viteri, Coal and syngas fueled power generation systems featuring zero atmospheric emissions, US Patent App 2003/0131582 A1 (2002).
[47] R.A. Geisbrecht, M.C. Williams, Fuel cell hybrid system, US Patent 6,623,880 (2003).
[48] P.L. Micheli, M.C. Williams, A.F. Sudhoff, Indirect-fired gas turbine dual fuel cell power cycle, US Patent 5,541,014 (1996).
[49] S.D. Labinov, T.R. Armstrong, R.R. Judkins, Fossil fuel combined cycle power generation method, US Patent App. 2007/0020492 A1 (2006).
[50] W.D. Seider, J.D. Seader, D.R. Lewin, S. Widago, Product and Process Design Principles, third ed., Wiley, Hoboken, NJ, 2009, pp. 534–597.
[51] L.B. Younis, J. Energy Inst. 79 (2006) 222–227.
[52] M.S. Peters, K.D. Timmerhaus, Plant Design and Economics for Chemical Engineers, fourth ed., McGraw-Hill, New York, 1991, pp. 438–439.
[53] J.R. Rostrup-Nielsen, J. Catal. 31 (1973) 173–199.
[54] K. Jarosch, T. El Solh, H.I. de Lasa, Chem. Eng. Sci. 57 (2002) 3439–3451.
[55] M.C. Williams, J.P. Strakey, W.A. Surdoval, U.S. DOE solid oxide fuel cells: technical advances, in: Proceedings of the 207th Meet. Electrochem. Soc., 2005, p. 1025.
[56] Energy Information Administration, Annual Energy Outlook 2009 With Projections to 2030, US DOE/EIA-0383, 2009.
[57] U.S. Environmental Protection Agency, Technical Development Document for the Final Regulations Addressing Cooling Water Intake Structures for New Facilities, EPA-821-R-01-036, 2001.
[58] L. Duan, R. Lin, S. Deng, H. Jin, R. Cai, Energy Convers. Manage. 45 (2004) 797–809.
[59] S. Shelly, Chem. Eng. Prog. 105 (2009) 1.
[60] Ø. Brandvoll, O. Bolland, J. Eng. Gas Turb. Power 126 (2004) 316–321.
[61] T.A. Adams, P.I. Barton, Int. J. Hydrogen Energy 34 (2009) 8877–8891.